Supplementary Information (SI) for Materials Horizons.
This journal is © The Royal Society of Chemistry 2025

Supplementary information 1

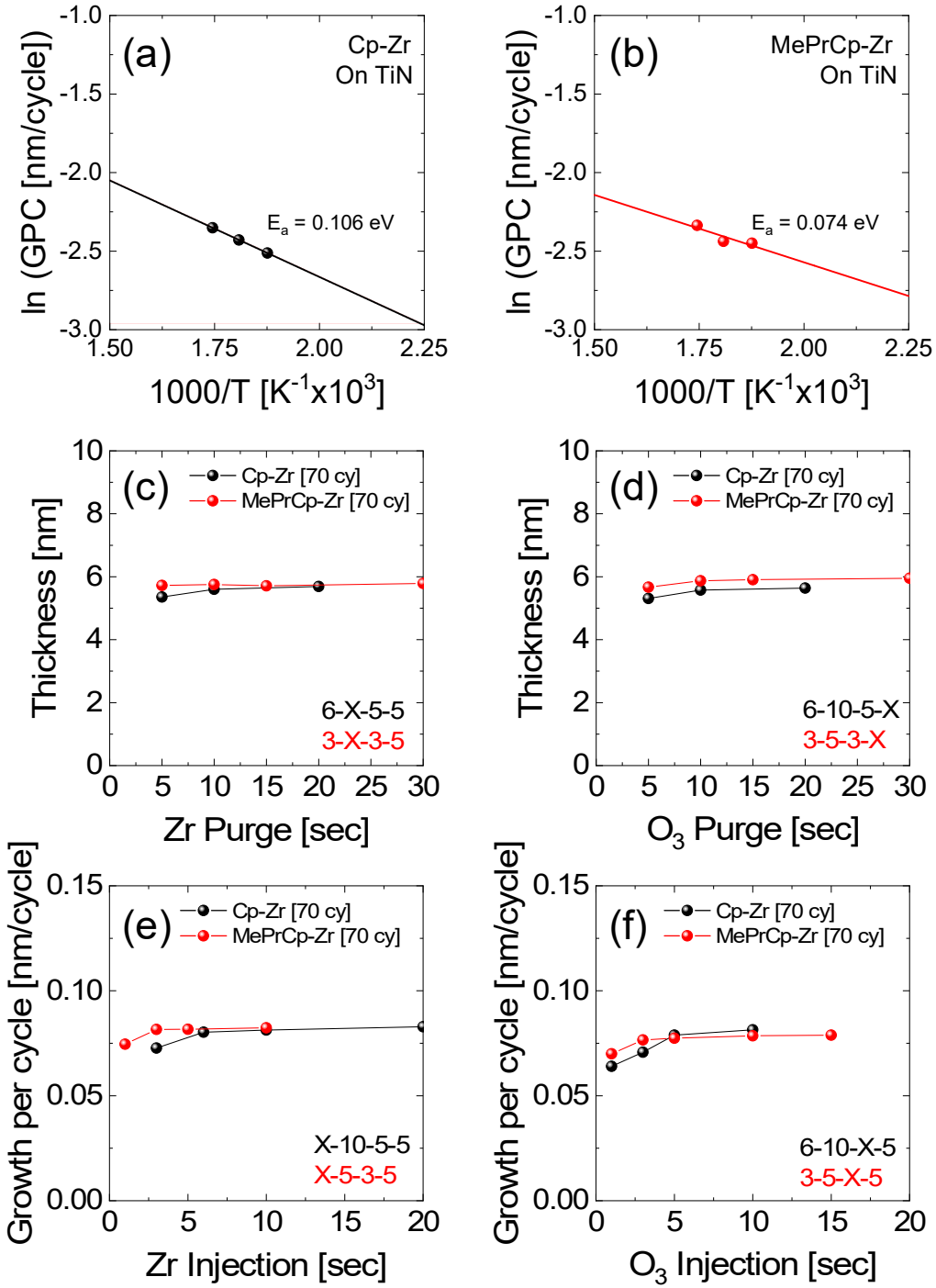

Fig. S1 Arrhenius plots comparing the activation energies (Ea) of (a) Cp-Zr and (b) MePrCp-Zr precursors, obtained from the temperature-dependent growth per cycle on TiN substrates. The data points correspond to deposition temperatures of 260 °C, 280 °C, and 300 °C. The extracted activation energies were 0.106 eV for Cp-Zr and 0.074 eV for MePrCp-Zr, respectively. The lower E_a value of MePrCp-Zr indicates that surface reactions occur more readily within the same temperature range, attributed to the partial methyl substitution in the ligand, which facilitates ligand dissociation from the Zr center and enhances surface reactivity. Consequently, MePrCp-Zr exhibits shorter saturation times and lower activation energy than Cp-Zr, clearly demonstrating its higher reactivity and improved ALD kinetics. Variations in the ZrO_2 film thickness as a function of (c) precursor purge time and (d) O_3 purge time, both on Si substrates. ALD saturation behavior was evaluated by varying one of the four process steps. In terms of precursor purge time, saturation was observed at 10 s and 5 s for the Cp-Zr and MePrCp-Zr precursors, respectively. In the case of O_3 purge time, saturation was confirmed at 5 s for both precursors. Variations in the growth per cycle of ZrO_2 film thickness as a function of (e) precursor injection time and (f) O_3 injection time, both on Si substrates.

Supplementary information 2

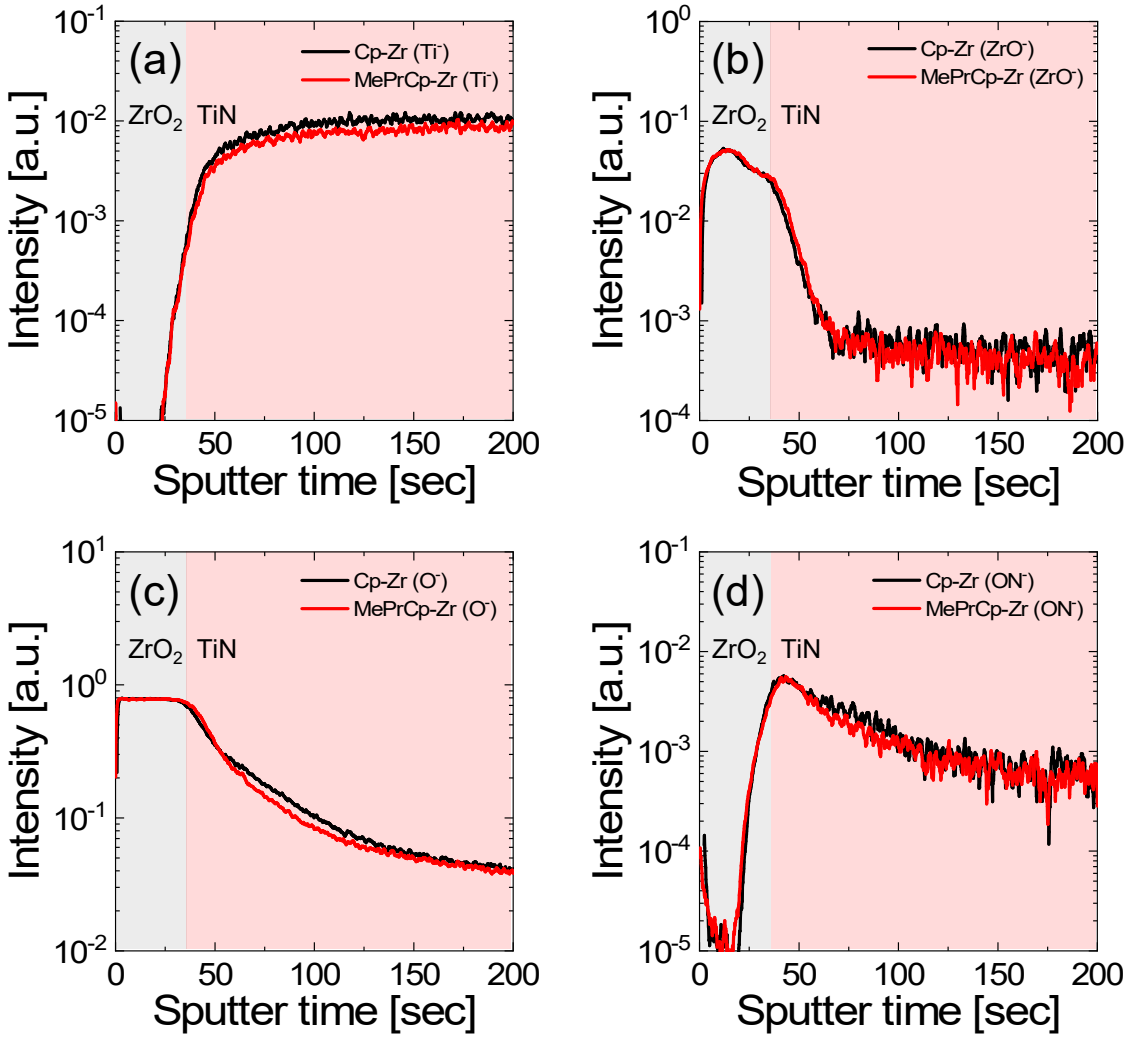

Fig. S2 ToF-SIMS depth profiles of 10 nm ZrO_2/TiN samples using Cp-Zr and MePrCp-Zr precursors. The analysis was conducted to compare the oxidation states of the TiN electrodes at the ZrO_2/TiN interfaces by detecting Ti^-, ZrO^-, O^-, and ON^- ion signals. In particular, the O^- and ON^- signals presented were used as direct indicators of the oxidation degree of the TiN electrode. After the region where the ZrO^- intensity sharply decreases and the ON^- intensity rapidly increases, the signals correspond to the TiN surface. The MePrCp-Zr precursor exhibited distinctly lower O^- and ON^- intensities than the Cp-Zr precursor within the TiN region, indicating that MePrCp-Zr effectively suppresses and partially reduces excessive oxygen reactions on the TiN surface.

Supplementary information 3

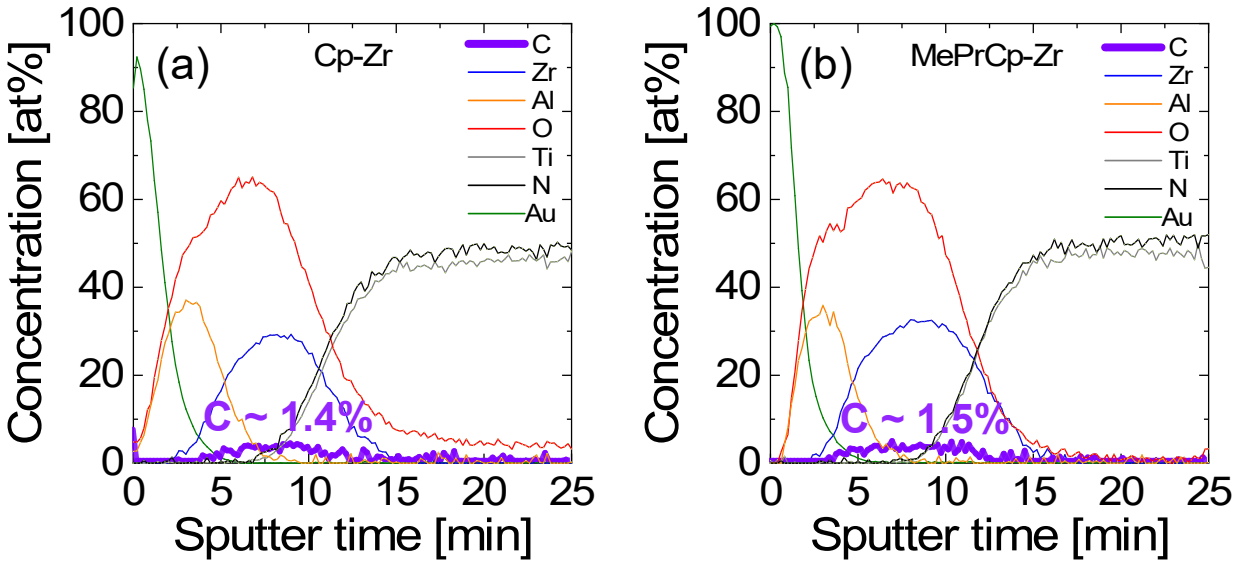

Fig. S3 AES depth profiles of Au/4 nm Al_2O_3/8 nm ZrO_2/TiN samples using (a) Cp-Zr and (b) MePrCp-Zr precursors. Both films exhibited low carbon impurity of approximately 1.5% within the ZrO_2 layers. The detected carbon is likely associated with residual ligand species that were not fully removed during film growth. These results indicate that both precursors enable the formation of ZrO_2 films with acceptable carbon impurity levels for dielectric applications.

Supplementary information 4

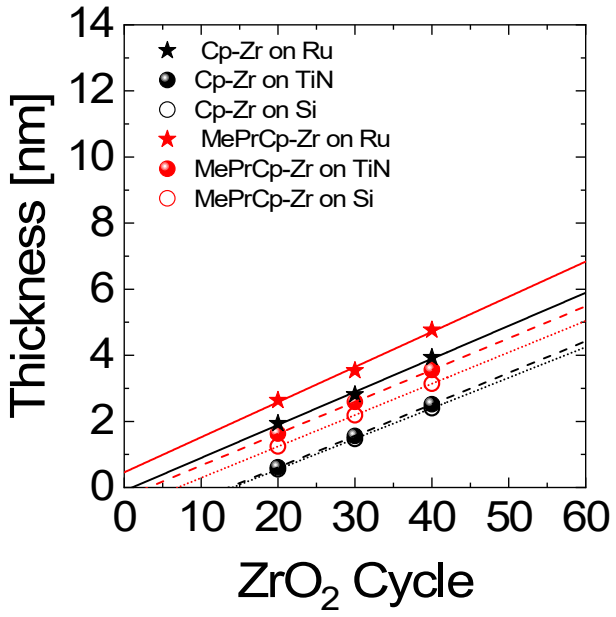

Fig. S4 Comparison of the growth behavior of ZrO_2 films deposited using Cp-Zr (injection time: 6 s–10 s–5 s–5 s) and MePrCp-Zr (injection time: 3 s–5 s–3 s–5 s) precursors on Ru, Si, and TiN substrates. The ZrO_2 films were deposited for 20, 30, and 40 cycles, and the MePrCp-Zr precursor exhibited faster ZrO_x nucleation compared to the Cp-Zr precursor.

Supplementary information 5

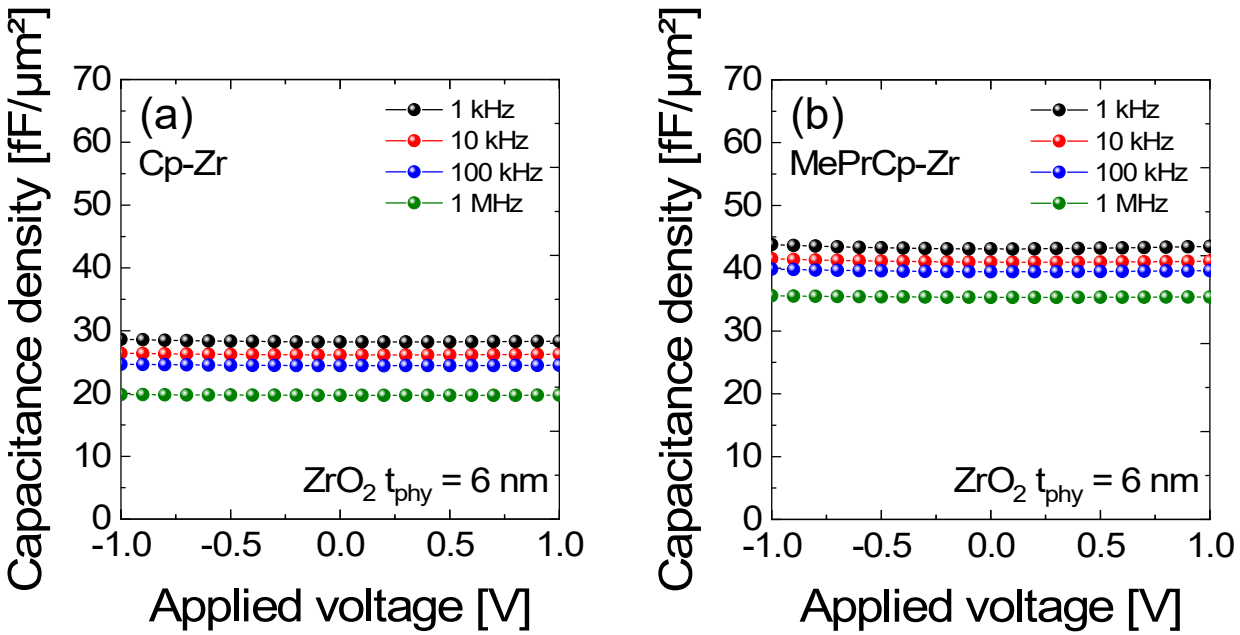

Fig. S5 Capacitance density as a function of applied voltage for Pt/6 nm ZrO_2/TiN capacitors using Cp-Zr and MePrCp-Zr precursors. Both samples exhibited stable and nearly flat C–V curves over the frequency range from 1 kHz to 1 MHz, and the MePrCp-Zr-based capacitor maintained a higher capacitance density than the Cp-Zr-based one across all frequencies.

Supplementary information 6

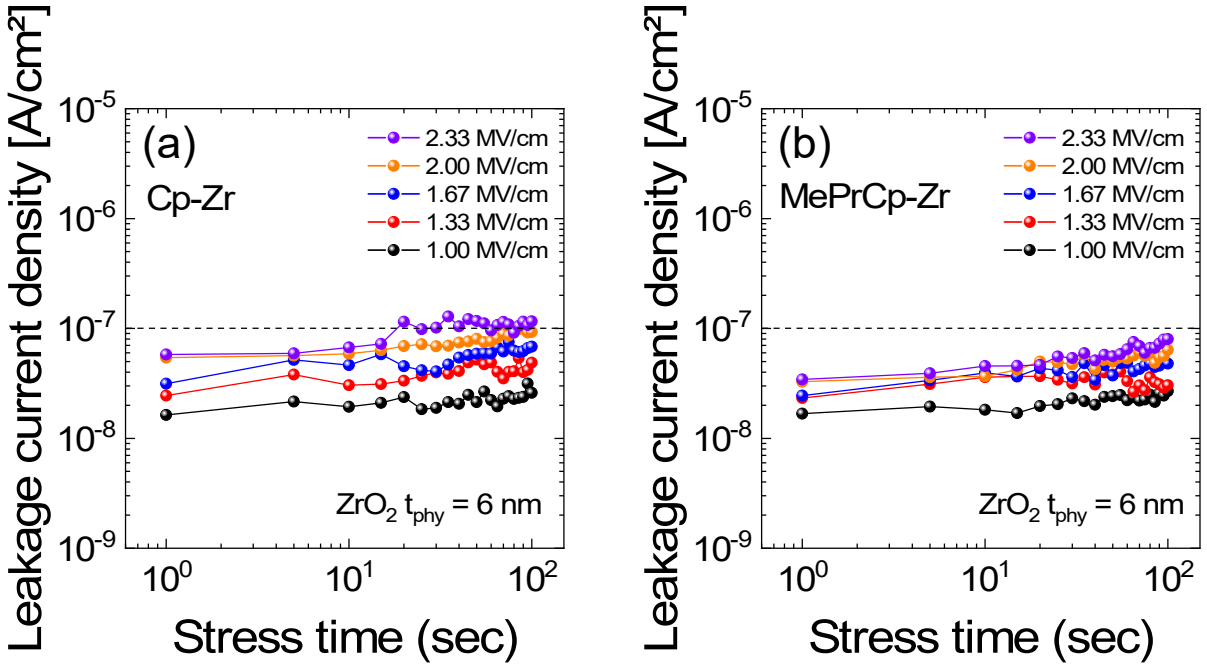

Fig. S6 Leakage current density as a function of stress time for Pt/ZrO_2/TiN capacitors with 6 nm ZrO_2, deposited using (a) Cp-Zr and (b) MePrCp-Zr precursors. The stress electric fields were applied in the range of 1.00–2.33 MV/cm, and the stress duration was measured up to 10^2 s.

Supplementary information 7

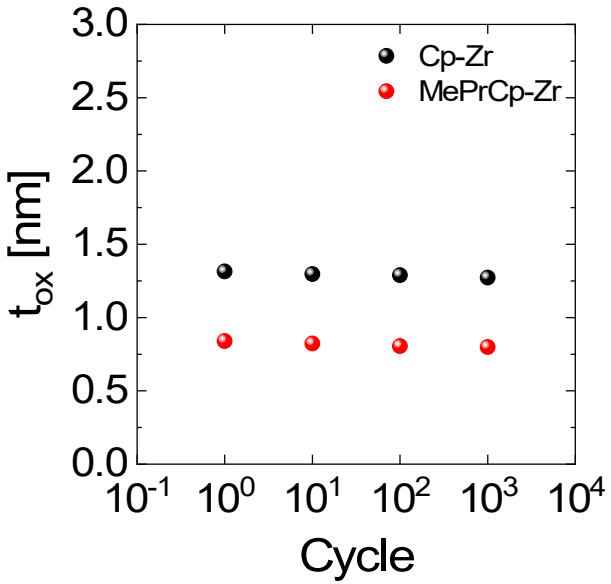

Fig. S7 Endurance cycling properties of Pt/ZrO_2/TiN capacitors deposited using Cp-Zr and MePrCp-Zr precursors. Bipolar voltage pulses as high as ±1 V were applied to evaluate endurance cycles. No significant change in t_{ox} was observed up to 10^3 cycles, indicating that both capacitors maintained stable operation under repetitive electrical stress.

Supplementary information 8

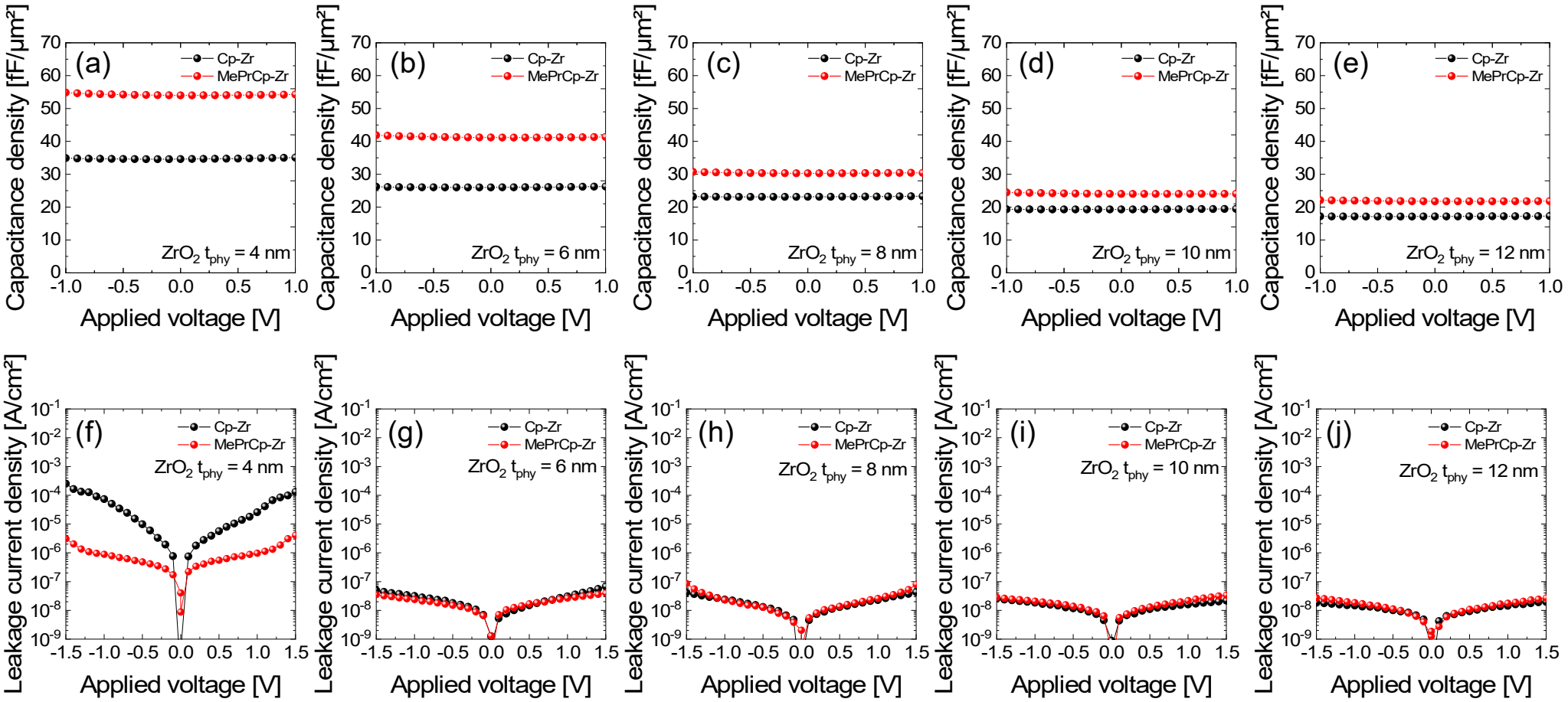

Fig. S8 Capacitance density as a function of applied voltage for Pt/ZrO_2/TiN capacitors with ZrO_2 thicknesses of (a) 4 nm, (b) 6 nm, (c) 8 nm, (d) 10 nm and (e) 12 nm, deposited using Cp-Zr and MePrCp-Zr precursors. Leakage current density as a function of applied voltage of Pt/ZrO_2/TiN capacitors with ZrO_2 thicknesses of (f) 4 nm, (g) 6 nm, (h) 8 nm, (i) 10 nm and (j) 12 nm, also deposited using Cp-Zr and MePrCp-Zr precursors. MePrCp-Zr precursor consistently exhibited higher capacitance density across all thicknesses compared to Cp-Zr, as a result of reduced interfacial layer formation during the early stages of ZrO_2 growth.